Available online at www.sciencedirect.com
ScienceDirect
Thermochimica Acta 456 (2007) 134–144
thermochimica acta
www.elsevier.com/locate/tca

Effect of zinc borate on the thermal degradation of ammonium polyphosphate

F. Samyn, S. Bourbigot*, S. Duquesne, R. Delobel

Laboratoire Procédés d'Elaboration des Revêtements Fonctionnels (PERF), LSPES – UMR 8008, Ecole Nationale Supérieure de Chimie de Lille (ENSCL), Avenue Dimitri Mendeleïev – Bât. C7, BP 90108, 59652 Villeneuve d'Ascq Cedex, France

Received 17 November 2006; received in revised form 9 February 2007; accepted 9 February 2007
Available online 16 February 2007

Abstract

The thermal behaviour of a mixture containing an ammonium polyphosphate based compound (AP760) and zinc borate (ZB) is investigated. After an investigation of the degradation of the pure components, the interactions between them are examined by thermogravimetry. Then, X-ray diffraction (XRD) and ^{11}B and ^{31}P solid-state nuclear magnetic resonance (NMR) measurements have been carried out on residues of mixtures of AP760 and FBZB heat treated at different characteristic temperatures. It reveals the nature of the interactions taking place between the two components. It is demonstrated that reactions lead to the formation of zinc phosphate and of borophosphates. Mechanisms of thermal degradation are proposed.

Keywords: Zinc borate; Ammonium polyphosphate; Zinc borate; ^{11}B–^{31}P solid state NMR; Thermal degradation; X-ray diffraction

1. Introduction

Metal borates are of considerable interest due to their rich structural chemistry and find extensive industrial use [1–5]. Among the wide variety of existing metal borates, zinc borates, compounds with the chemical composition of xZnO, $y$$B_2O_3$, $z$$H_2O$ are used since 1940 [6]. Today the most important commercial zinc borate (Firebrake® ZB (ZB) = 2ZnO, 3B_2O_3, 3H_2O), introduced more than 30 years ago, finds a particular application as polymer additive.

This use in polymers have rise great interest among the scientists and particularly in the fire retardant field. Indeed, it can be used with a wide range of polymeric matrices (PVC, polyolefins, elastomers, polyamides or epoxy resins) mainly in conjunction with traditional fire retardant additives (halogen-containing and halogen-free systems including alumina trihydrate, magnesium hydroxide, red phosphorus or ammonium polyphosphate). Moreover, its action as smoke suppressants, afterglow suppressants, corrosion inhibitors, and synergistic agent has been pointed out [7–9].

The properties achievable using ZB are well described particularly when used with metal hydroxide compounds. As an example, zinc borates can act as synergistic agents in ethylene-vinyl acetate copolymer/metal hydroxide based formulations [10–12]. It has been demonstrated that the addition of small amount of ZB sharply affects the structure, the expansion and the mechanical resistance of the ceramic like protective layer resulting in better fire retardant performance. Moreover, it has been proved that zinc borate in a polymer promotes the formation of char. If the combination of metal hydroxide with ZB has been extensively studied, less is known about zinc borate used in intumescent formulations. Intumescent formulations are complex systems for flame retarding polymers. They contain at least three ingredients [13]: an acid source, a carbonisation compound and a blowing agent. The mechanism of action can be described as follows: (i) the acid source breaks down to yield a mineral acid; (ii) then it takes a part in the dehydration of the carbonific to yield the carbon char; and (iii) finally the blowing agent decomposes to yield gaseous products. This causes the char to swell and hence provides the insulating material which then decomposes under the action of the outer heat flux at high temperature. The mechanism is so based on slowing down heat and mass transfer between the gas phase and the condensed phase. With the incorporation of ZB in such formulations, a significant improvement of the fire

* Corresponding author. Tel.: +33 3 20 43 48 88; fax: +33 3 20 43 65 84.
E-mail address: serge.bourbigot@ensc-lille.fr (S. Bourbigot).

0040-6031/$ – see front matter © 2007 Elsevier B.V. All rights reserved.
doi:10.1016/j.tca.2007.02.006

behaviour is observed [14] but the understanding of their mode of action is not fully understood and it should be investigated.

In our laboratory, it has been shown that the combination of ammonium polyphosphate (APP) based compound (intrinsic intumescent formulation) and ZB in polypropylene (PP) leads to a synergistic effect in terms of fire behaviour (according to the limited oxygen index (L.O.I.) test (ASTM D2863/77 Philadelphia PA American Society for Testing and Materials 1977)) (manuscript in preparation). Consequently investigations on the thermal degradation of APP/ZB mixtures have been carried out in order to explain this observation. First the degradation of the two components will be investigated separately and then the thermal behaviour of a mixture containing 50% of APP and 50% ZB will be examined. The ratio 50/50 was selected to have enough of each compound to detect the interactions. In the three cases the same procedure of investigation will be used: (i) first thermogravimetric analyses will be performed to examine the thermal behaviour of the compound; (ii) then characteristic temperatures (heat treatment temperature: HTT) will be determined according to the TG curves and the samples will be heat-treated isothermally for 3 h in air; (iii) the residues so prepared will be analysed (XRD and solid state ^{31}P and ^{11}B NMR); and (iv) finally on the basis of these analyses mechanisms of degradation will be suggested.

2. Experimental

2.1. Materials

Exolit AP760 (AP760), an ammonium polyphosphate (APP) derivative was supplied by Clariant. It is an APP coated with a component containing nitrogenous and carbonaceous species (characteristics: 20 (w/w)% P, 14(w/w)% N, 0.5% water).

A commercial grade of zinc borate Firebrake® ZB (ZB) was supplied by Luzenac. The formula typically used to describe this material as a commercial grade is 2ZnO, $3B_2O_3$, $3.5H_2O$ but recently Schubert et al. [6] suggested that the correct formula is 2ZnO, $3B_2O_3$, $3H_2O$ (this formula will be used in the following).

2.2. Thermal analyses

Thermogravimetric (TG) analyses were carried out at a heating rate of 10 °C/min in synthetic air flow (flow rate: 30 mL/min, air liquid grade) using a Setaram 92-16 microbalance. Samples of about 10 mg are analysed in opened silica pans.

Interactions between the compounds of a mixture can be revealed by comparing the experimental TG curve with a "theoretical" TG curve (W_{theo}) calculated as a linear combination of the TG curves of the mixture ingredients weighted by their contents

$$W_{theo}(T) = \sum_{i=1}^{n} x_i W_i(T)$$

where x_i: content of compound I and W_i: TG curve of the compound i.

In order to determine the potential interactions between the two components and their further effects on the thermal stability of the systems, the curves of weight differences between experimental and theoretical TG curves were computed as follows

$$\Delta W(T) = W_{exp}(T) - W_{theo}(T)$$

where $\Delta W(T)$: curve of weight difference and $W_{exp}(T)$: experimental TG curve of the formulation.

2.3. Thermal treatments

According to TG curves of the compounds and mixtures of them, five temperatures characteristic of the different steps of degradation (heat treatment temperature: HTT) have been determined (260, 360, 415, 580 and 800 °C). Thermal treatments have been carried out at these temperatures in order to simulate the evolution of the intumescent process and to investigate the structure of the intumescent char and its composition. At the selected temperature, the sample is put in the tubular furnace and undergoes the thermal treatment for 3 h in air. The so prepared samples are kept in a desiccator in vacuum until further analyses.

2.4. XRD analysis

XRD spectra were recorded in the 5°–60° 2θ range using a Brucker AXS D8 diffractometer ($\lambda_{(Cu\ K\alpha)}$ = 1,5418 Å, 40 keV, 25 mA) in configuration 2-theta/theta. The acquisition parameters were as follows: a step of 0.02°, a step time of 2 s. The data are analysed using the diffraction patterns of inorganic crystal structure database (ICSD) [15].

2.5. Solid state NMR measurements

^{13}C NMR measurements were performed on a Bruker ASX100 at 25.2 MHz (2.35T) with MAS (magic angle spinning) and ^{1}H-^{13}C cross polarisation (CP) using a 7 mm probe. For all samples, a repetition time of 5 s, a contact time of 1 ms and a spinning speed of 10 kHz were used. All spectra are acquired as the result of 1024 scans. The reference used was tetramethylsilane (TMS).

^{31}P NMR measurements were performed on a Bruker ASX400 at 40.5 MHz (9.4T) with MAS using a 4 mm probe. For all samples, a repetition time of 450 s and the spinning speed of 5 kHz were used. All spectra are acquired as the result of 16 scans. The reference used was 85% H_3PO_4 in aqueous solution.

^{11}B NMR measurements were performed on the same spectrometer as before at 128.3 MHz (9.4T) with MAS using a 4 mm probe. For all samples, a repetition time of 10 s and the spinning speed of 15 kHz were used. All spectra are acquired as the result of 32 scans The reference used was $(C_2H_5)O,BF_3$. The simulations of the spectra were made using the software Quasar [16].

3. Results and discussion

3.1. Degradation of AP760

3.1.1. TG analysis

AP760 degrades in a three steps process (Fig. 1): a first step between 200 and 360 °C corresponding to about 22% weight loss, a second between 360 and 420 °C corresponding to about 12% weight loss and the third between 580 and 620 °C leading to material that slowly degrades up to 800 °C.

AP760 is an ammonium polyphosphate (APP) which contains a synergistic agent that includes carbon and nitrogen (isocyanurate based compound). The degradation of a pure APP has already been described in the literature [17] as a two steps process (Fig. 1). The first step, which starts at about 300 °C, corresponds to the release of ammonia and water. The resulting degradation products crosslink in a highly condensed polyphosphoric acid. During the second step, which starts at about 550 °C, the evolution of polyphosphoric acid and/or a dehydration of the acid to P_4O_{10}, which sublimates, is suggested. A comparison between the thermal behaviour of the neat APP and the AP760 shows that the degradation of AP760 occurs at lower temperature. To explain this difference, two assumptions can be made: (i) the degradation of the nitrogenised compound occurs at lower temperature than APP and/or (ii) a reaction between APP and this compound occurs before the degradation of the APP leading to evolving gaseous products.

3.1.2. Thermal treatment

A description of the residues is given in Table 1. The AP760 supplied as a white powder yields upon heating at 260 °C a light brown powder. At 360 and 415 °C the formation of a foamed expanded charred structure is observed. Above 415 °C, the residue is no longer black but exhibits a crumbly white solid aspect. It suggests a significant evolution of the chemical composition of the product upon heating. It is examined using appropriate spectroscopic tools in the next section.

Table 1
Description of the isothermally heat-treated samples

HTT (°C)	Residual mass (wt.%)	Resulting material
AP760		
260	90	Light brown powder
360	73	Black foam
415	60	Black foam
580	25	Crumbly white solid
800	20	Crumbly white solid
ZB		
260	100	White powder
360	92	White powder
415	85	White powder
580	85	Crumbly white solid
800	84	Tough white solid
260	95	Light brown powder
AP760/ZB		
415	74	Black powder
580	69	Black powder
800	69	White powder

3.1.3. Spectroscopic analyses

XRD spectra of AP760 at the different HTT are presented on Fig. 2. The powder at 20 °C and the residue of the treatment at 260 °C have the same spectrum which is characteristic of ammonium polyphosphate form crystalline II. There are mainly five crystalline forms of APP. The crystalline form I is obtained by heating an equimolar mixture of ammonium orthophosphate and urea under ammonia at 280 °C. The crystalline form II, which presents an orthorhombic symmetry ($a = 4.256$ Å; $b = 6.475$ Å; $c = 12.04$ Å) and belongs to the $P2_12_12_1$ spatial group [18], can be easily obtained when heating up the form I between 200 and 375 °C. The form III is an intermediate form which appears during the transition form I to form II. The form IV has a monoclinic structure whereas the form V is orthorhombic. Only the forms I and II are commercially available. After the treatment at 415 °C, the residue exhibits a charred structure and its spectrum is made of a broad band (22–23° 2-theta values) suggesting

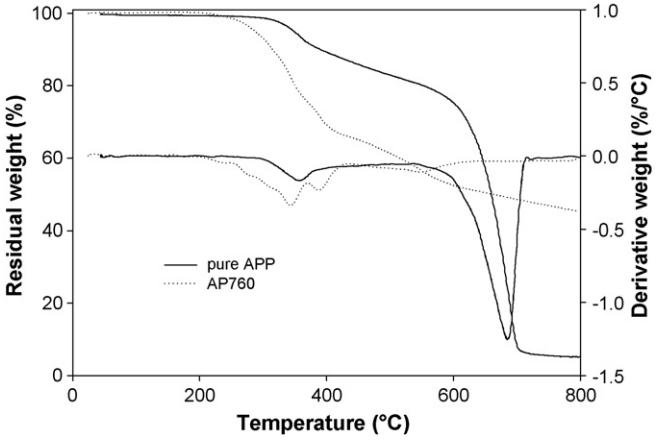

Fig. 1. TG curves (upper curves) and its derivative (down curves) of AP760 and pure APP (10 °C/min, air flow).

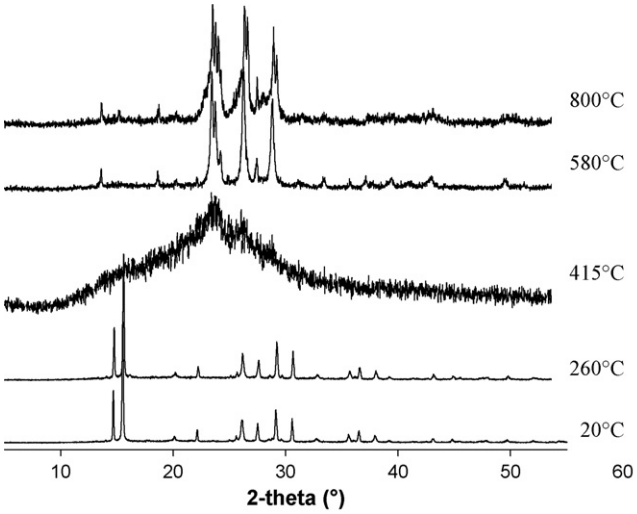

Fig. 2. XRD spectra of the residues of AP760 at the different HTT.

the formation of an amorphous product containing pregraphitic carbon [19,20]. For HTT of 580 and 800 °C, a SiO_2–P_2O_5 phase (formation of silicophosphate species) has been identified. This might be explained by the presence of SiO_2 in the AP760 (the exact composition of AP760 is unknown but we suspect that SiO_2 or some derivatives might be used as synergistic agent).

3.1.4. MAS NMR ^{31}P characterisation

Solid state NMR is a powerful tool to characterise the residues however those exhibiting a "paste" cannot be analysed because the high spinning speed throwing out the sample of the rotor (samples heat treated at 360 and 415 °C).

^{31}P NMR has been performed in order to characterize the evolution of phosphate species in the residues of the different thermal treatments (Fig. 3). Those results confirm the degradation mechanism of polyphosphate widely reported in the literature. At room temperature the characteristic spectrum of APP with the two bands at −22 ppm and −24 ppm is observed [21–23]. At 260 °C, two different sites of phosphate species are revealed on the spectrum. The doublet can be attributed to the polyphosphate units (it corresponds to the spectrum of APP at 20 °C) while the band at around 0 ppm is characteristic of orthophosphate groups and/or phosphoric acid [21–23]. At higher temperatures (580 and 800 °C) only condensed species are detected (broad band centred at −50 ppm assigned to disordered crosslinked polyphosphoric acid) [21–23].

3.1.5. Proposed mechanism of degradation

According to our analyses, the mechanism of degradation of AP760 can be explained as follows. First at about 250 °C ammonium polyphosphate decomposes to yield polyphosphoric acid and evolving ammonia (first step of the TG curve) (Eq. (1)).

$$[NH_4PO_3]_n \rightarrow [HPO_3]_n + nNH_3 \quad (1)$$

Between 360 and 420 °C, the polyphosphoric acid reacts with the carbonaceous compound to form the char (phosphocarbonaceous structure described in the literature [24]) and with the release of water and ammonia the intumescence process occurs (Eq. (2)).

$$[HPO_3]_n + \text{Carbon source} \rightarrow \text{C} + H_3PO_4 \quad (2)$$

It explains that at both temperatures, the residues obtained at 360 and 415 °C were black foams. The fatty aspect of these foams can be attributed to the formation of phosphoric acid at this stage of the degradation. At higher temperatures the intumescent structure degrades totally and cross linked polyphosphoric acid is formed what explains the white powders obtained at 580 and 800 °C. Phosphorus oxides might be trapped into the network and so, are not sublimated.

3.2. Degradation of ZB

3.2.1. TG analysis

TG analysis of ZB is reported in Fig. 4. The thermal degradation of ZB occurs in two steps: a first step between 300 and 360 °C corresponding to a weight loss of about 5% and a second step between 360 and 430 °C leading to a thermally stable material (88 wt.% of the initial mass). The 12 wt.% weight loss may be attributed to loss of water (Eq. (3)).

$$2ZnO,\ 3B_2O_3,\ 3H_2O \rightarrow 2ZnO,\ 3B_2O_3 + 3H_2O \quad (3)$$

3.2.2. Thermal treatment

The same thermal treatments as in the case of AP760 have been carried out. The aspect of the residues obtained is presented in Table 1. Practically no evolution can be observed between the residues. Below 580 °C, at each HTT a white powder is obtained and at higher temperature the powder agglomerates to lead at 580 °C a crumbly white solid and at 800 °C a though white solid.

3.2.3. XRD analyses

XRD spectra of untreated ZB and of the heat treated residues are reported in Fig. 5. The XRD spectra corresponding to HTT below 360 °C are similar. At 415 °C the product exhibits an amorphous character. The product obtained at 580 °C presents

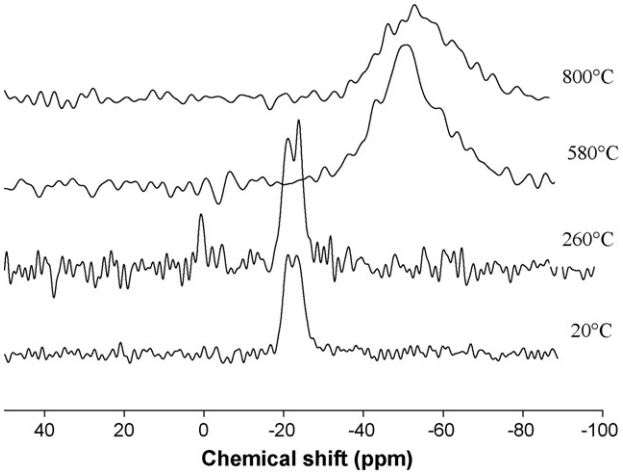

Fig. 3. DD-MAS ^{31}P NMR analyses of AP760 at the different HTT.

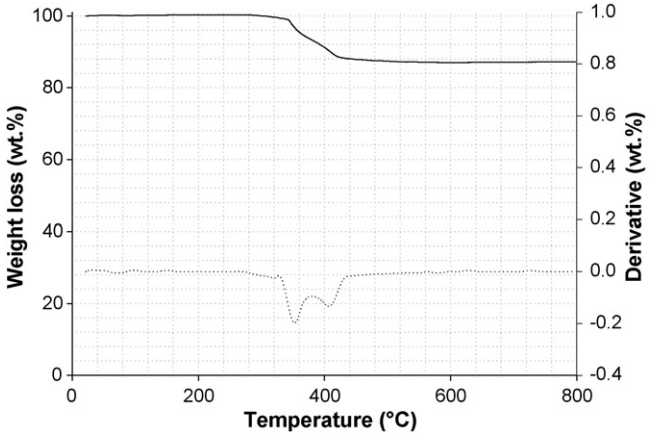

Fig. 4. TG curve of ZB.

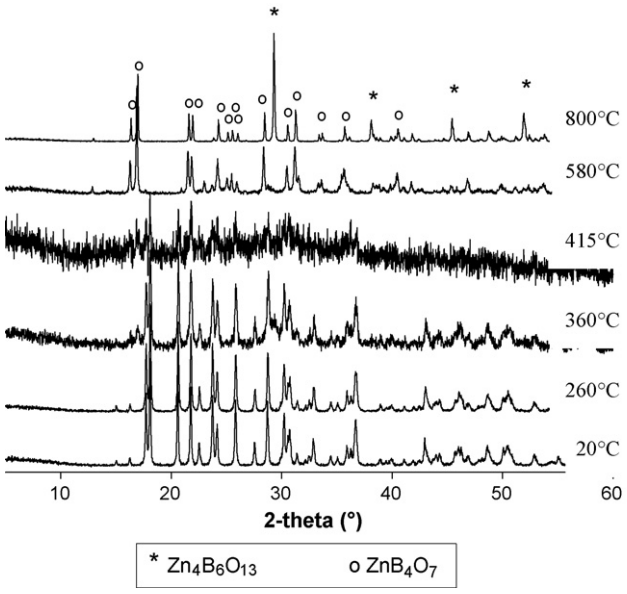

Fig. 5. XRD spectra of the residues of ZB at the different HTT.

a spectrum different from those at 260 and 360 °C. ZnB_4O_7 specie has been identified in this crystalline structure. However, since the Zn/B ratio is equal to 1/4 compare to 1/3 in ZB, it suggests the presence of other phases in the structure (probably amorphous since they are not detected by X-ray diffraction analysis). Finally, for the residue of powder treated at 800 °C, two crystalline forms are detectable: ZnB_4O_7 and $Zn_4B_6O_{13}$.

3.2.4. MAS NMR ^{11}B characterisation

Solid state ^{11}B NMR has become a key technique in the characterisation of the borates and borate glasses. In fact, thanks to this technique BO_3 and BO_4 units, constituents of borate species, can be distinguished by their ^{11}B quadrupolar coupling parameters [25–27], which reflect the interaction between the nuclear electric quadrupolar moment (Q) and the electric field gradient (EFG) tensor (V_{ij}) at the nuclear site. The quadrupolar coupling tensor can be expressed by the quadrupolar coupling constant $C_Q = eQV_{zz}/h$, and the asymmetry parameter $\eta_Q = (V_{yy} - V_{xx})/V_{zz}$ which describe the magnitude and symmetry of interaction, and thereby the distortion of the local BO_3 and BO_4 units. Generally, BO_4 tetrahedra in borates exhibits C_Q values less than 1 MHz whereas BO_3 groups possess quadrupolar couplings in the range $2.4 \leq C_Q \leq 3.0$ MHz [28–34]. Furthermore, the two types of boron surroundings can be distinguished by the ^{11}B isotropic chemical shifts (δ_{iso}) because BO_3 units resonate in the range $12 \leq \delta_{iso} \leq 25$ ppm, whereas BO_4 groups exhibit shifts in the approximate range $-4 \leq \delta_{iso} \leq 6$ ppm. Separate resonances for BO_3 and BO_4 can be then achieved and so a quantification of these species in borates species can be done simulating the spectra.

Fig. 6 shows the ^{11}B NMR spectrum of the sole ZB. It exhibits a typical quadrupolar lineshape [35] which has been simulated.

To see the evolution of the boron species versus the HTT, the ^{11}B NMR spectra of all the residues have been recorded (Fig. 7) and simulated taking into account the quadrupolar parameters of the neat ZB as reference.

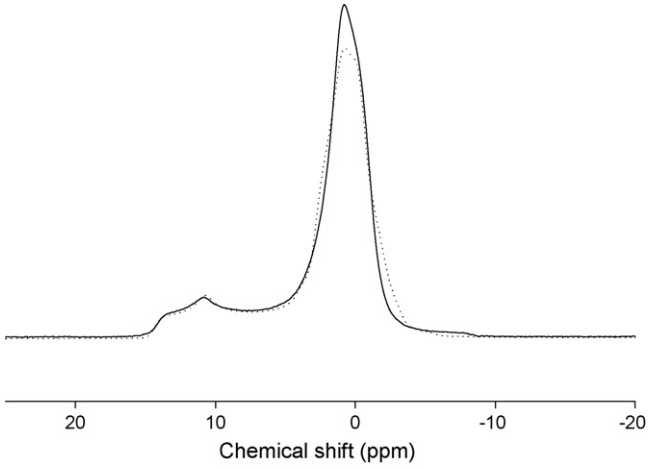

Fig. 6. MAS ^{11}B NMR spectrum of ZB (solid line: experimental spectrum; dotted line: simulated spectrum).

Table 2 summarizes the values of the different parameters used to fit the experimental curves at each HTT. A graphic representation of the concentration of the boron species versus the temperature is given in Fig. 8. These simulations reveal the presence of boron atoms in both trigonal (BO_3) and tetragonal (BO_4) bonding configurations at the five temperatures in different ratios. At 580 and 800 °C, two distinct types of BO_3 units are formed. This can be explained by a different surrounding of the BO_3 units.

3.2.5. Proposed mechanism of degradation

According to our analyses, a mechanism of degradation can be proposed. A work very similar to this presented here have been done by Schubert and al [6]. Indeed after thermal treatments on samples of ZB they proposed a mechanism of degradation. The degradation described by Schubert can be decomposed in three steps (Eqs. (4)–(6)) as our mechanism but with the formation of different intermediate products. We will compare step by

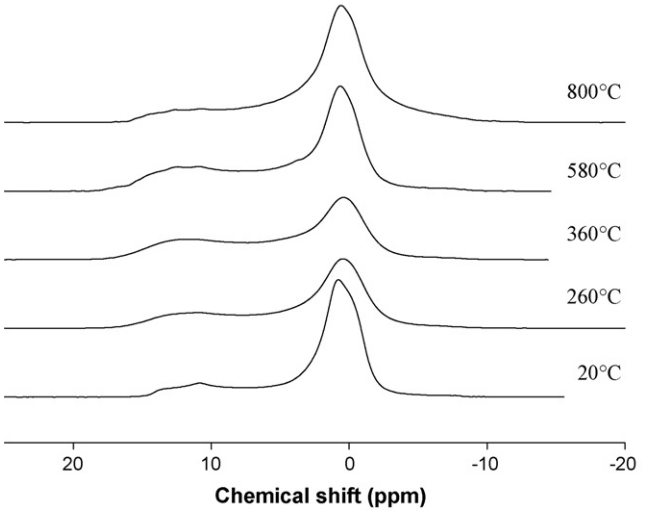

Fig. 7. DD-MAS ^{11}B NMR analyses of the residues.

Table 2
NMR parameters of the boron species present in ZB residues determined by simulation

ZB 20 °C		ZB 360 °C		ZB 415 °C		ZB 580 °C			ZB 800 °C		
BO_4	BO_3	BO_4	BO_3	BO_4	BO_3	BO_4	BO_3	BO_3 (2)	BO_4	BO_3	BO_3 (2)
R.C. (%)											
76	24	54	46	44	56	41	47	12	66	21	13
C_{iso} (ppm)											
1.9	16.2	2.0	17.4	2.0	17.4	2.2	18.0	13.7	3.2	15.7	17.7
C_Q											
0.9	2.4	1.0	2.6	0.9	2,6	1.0	2.6	2.4	1.3	2.4	2.4
η_Q											
0.7	0.3	0.7	0.3	1.0	0.3	0.7	0.3	0.9	0.7	0.9	0.4

R.C.: Relative concentration; C_{iso}: isotropic chemical shift; C_Q: quadripolar coupling constant; η_Q: quadripolar asymetry parameter.

step the two mechanisms.

$$2ZnO,\ 3B_2O_3,\ 3H_2O \rightarrow 2ZnO,\ 3B_2O_3 + 3H_2O \quad (4)$$

$$5(2ZnO,\ 3B_2O_3) \xrightarrow{640^\circ C} 2(3ZnO,\ B_2O_3) + 4ZnO,\ 3B_2O_3 + 10B_2O_3 \quad (5)$$

$$3ZnO,\ B_2O_3 + 4ZnO,\ 3B_2O_3 \xrightarrow{870^\circ C} \underset{\text{Evaporation}}{3ZnO,\ B_2O_3} + \underset{\text{cristalline}}{4ZnO,\ 3B_2O_3} \quad (6)$$

For Schubert, the first step consists in the condensation of the B–OH groups between 290 and 420 °C with release of water: the zinc borate degrades to yield an amorphous product which corresponds to its dehydrated form (Eq. (4)). This is consistent with the analyses we made notably with the TGA which shows the water loss in this range of temperature and the amorphous phase $2ZnO,\ 3B_2O_3$ was observed by XRD. The proportion of the BO_3/BO_4 units present in the zinc borate at 20 °C should be 1/2 according to the description of the crystal structure of the material [6] but the NMR analyses show a ratio of 1/3 and then the concentration of the two species converge to a main value of 1/2 along the dehydration. It tends to prove that the condensation results in the formation of BO_3 units and decrease of the BO_4 groups.

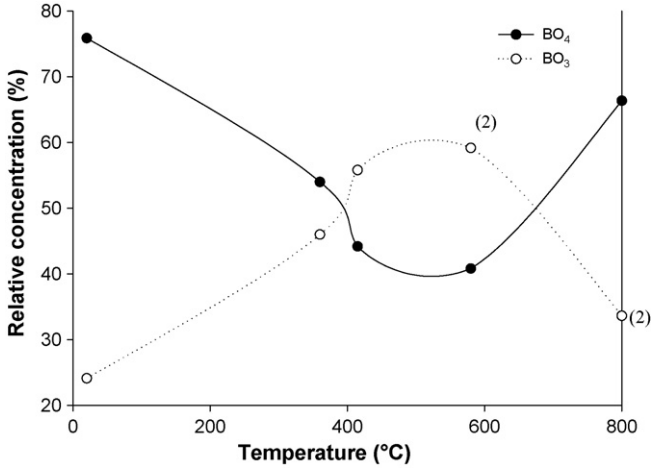

Fig. 8. Evolution of the relative concentration of boron species in ZB residues vs. temperature; (2) indicates that two different BO_3 species have been used in the simulation.

When Schubert describes the conservation of the compound $2ZnO,\ 3B_2O_3$ until 640 °C, our analyses show a modification of the structure from 420 °C up to 580 °C the compound degrades totally or partially to yield ZnO, $2B_2O_3$ and other phases which has not been identified at this time (as explained in the XRD section) (Eq. (7)).

$$2ZnO,\ 3B_2O_3 \xrightarrow{420^\circ C<T<580^\circ C} ZnO,\ 2B_2O_3 + \text{other phase non identified} \quad (7)$$

Two crystalline forms of ZnO, $2B_2O_3$ are described in the literature [36]: the α and the β forms. On one hand, α-ZnO, $2B_2O_3$ is built up from BO_3-triangle and BO_4-tetrahedra sharing common vertices. The two cristallographically independent tetrahedra and triangle form a $[B_4O_7]^{2-}$ unit which is repeated throughout the structure. Each zinc atom is surrounded by four close oxygen atoms arranged in irregular tetrahedra. On the other hand, β-ZnO, $2B_2O_3$, which is a metastable form obtained at high pressure or high temperature, consists exclusively from corner sharing BO_4 tetrahedra. According to this discussion we may assume that only the α-ZnO, $2B_2O_3$ should be formed. It is consistent with the ratio BO_3/BO_4 equalling 1 measured by NMR.

Then according to our results, between 580 and 800 °C, other reactions take place leading to the formation of two different compounds: the same as above, i.e. α-ZnO, $2B_2O_3$ but also the compound $4ZnO,\ 3B_2O_3$ (Eq. (8)).

$$ZnO,\ 2B_2O_3 + \text{other phase non identified} \xrightarrow{580^\circ C<T<800^\circ C} ZnO,\ 2B_2O_3 + 4ZnO,\ 3B_2O_3 \quad (8)$$

The formation of the last compound quoted has also been reported to be created at 640 °C by Schubert resulting from direct degradation of $2ZnO,\ 3B_2O_3$. In our case, the formation of $4ZnO,\ 3B_2O_3$ might result from the decomposition of ZnO,

$2B_2O_3$ as it has been described in the literature [36] (Eq. (9)).

$$4(\alpha - ZnO, 2B_2O_3) \overset{710^\circ C<T<900^\circ C}{\longrightarrow} 4ZnO, 3B_2O_3 + 5B_2O_3 \quad (9)$$

This decomposition has been observed at 900 °C (Bauer [37] and Huppertz and Heymann [36]) but also at 710 °C (Whitaker [38]). The difference in the temperature of decomposition can probably be attributed to longer heating times in the case of the lower temperature. $4ZnO, 3B_2O_3$, with his cubic structure, is built up by BO_4 tetrahedra linked together forming a three dimensional framework [36]. So the formation of this compound could explain the increase of BO_4 species observed at 800 °C and the decrease of BO_3.

3.3. Study of the degradation of the mixtures AP760/ZB

3.3.1. TG analysis

Thermal degradation of AP760/ZB mixtures of different ratios is investigated by TGA (Fig. 9). The choice of these ratios has been imposed for different reasons. The substitution of AP760 with 5 or 25% of ZB has been proposed because usually the synergy is observed at low loading. The ratio 50/50 has been studied to detect potential interactions occurring during the degradation of the mixture. The addition of ZB in the AP760 enhances the thermal stability as a function of the ZB content. Indeed it is noteworthy that the residues at 800 °C of the AP760/ZB systems (from 55 wt.% for the formulation 95/5 to 75 wt.% for the formulation 50/50) are much higher than the sole AP760 (40 wt.%) and much higher than residues that could be expected by linear combination. Moreover for all ratios, degradation starts at about 250 °C but the slope of the curves (degradation rate) decreases as ZB content increases what implies a retardation of the evolution of volatile products. It suggests that interactions might occur between ZB and AP760 when degrading, stabilizing phosphorus species.

In order to confirm the assumption suggested above, the curves of weight loss difference are plotted on Fig. 10. For the ratios 75/25 (w/w) and 50/50 (w/w), a slight destabilization is observed between 250 and 480 °C while the system

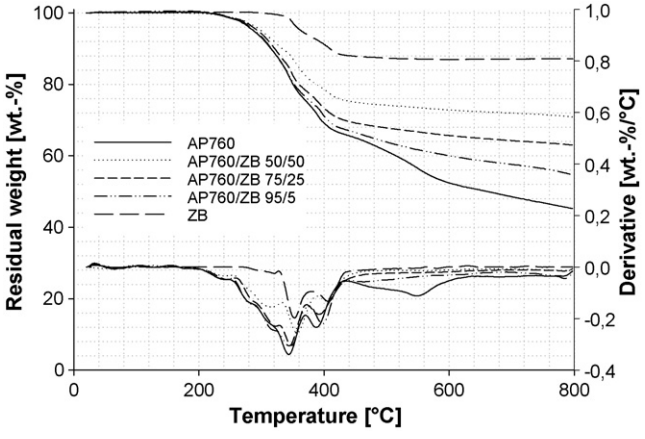

Fig. 9. TG curve of AP760, ZB and AP760/ZB mixture in different ratios (upper curves) in its derivatives (down curves) (10 °C/min, air flow).

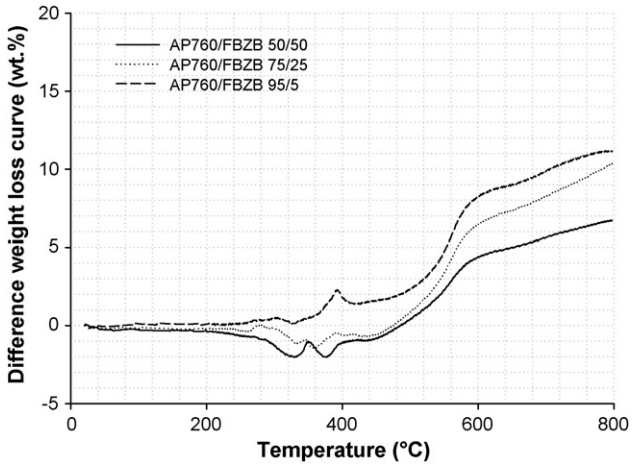

Fig. 10. Difference weight loss curves of mixture of AP760/ZB in different proportions.

95/5 (w/w) exhibits a stabilizing behaviour from room temperature till 800 °C. The stabilization of all these systems become efficient at high temperature ($T > 600$ °C) since the mass difference jumps to 7 wt.%, 10 wt.% and 12 wt.%, respectively for the ratios 50/50 (w/w), and 75/25 (w/w) and 95/5 (w/w).

3.3.2. Thermal treatment

As for the two previous compounds, thermal treatments at four temperatures have been carried out according to TG curves (260, 415, 580 and 800 °C) on mixture of 50% AP760 and 50% ZB. Descriptions of the residues are presented in Table 1. An evolution is observed between the heat treated samples. A light brown powder remains after the treatment at 260 °C, black powders are obtained at 415 and 580 °C and finally the residue at 800 °C is a white powder.

3.3.3. XRD analyses

Fig. 11 shows XRD spectra of the mixtures at different HTT. They reveal that reactions between AP760 and ZB start at 415 °C. At 580 °C BPO_4 and $Zn_2(PO_4)_2$ are detected suggesting that boron and zinc species react with phosphate to yield boron phosphate and zinc orthophosphate. At 800 °C, BPO_4 is still detected but zinc orthophosphate is transformed into zinc pyrophosphate ($Zn_2P_2O_7$). The formation of these compounds at high temperature might then explain the stabilization of phosphate species as suggested by TGA.

3.3.4. NMR characterisations

^{13}C, ^{31}P and ^{11}B NMR results of analyses on the residues of furnace treatments are respectively presented on Figs. 12–14. Different conclusions can be drawn according to these experiments.

^{13}C NMR measurements have been only carried out on the residues presenting a black colour because we suspected the formation of a char (carbonaceous structure). The residues heat treated at 415 and 580 °C were so analysed. In these two cases, the formation of char is confirmed (Fig. 12). The broad peak observed at around 130 ppm for the residue heat treated at 415 °C can be assigned to several types of aromatic and polyaromatic

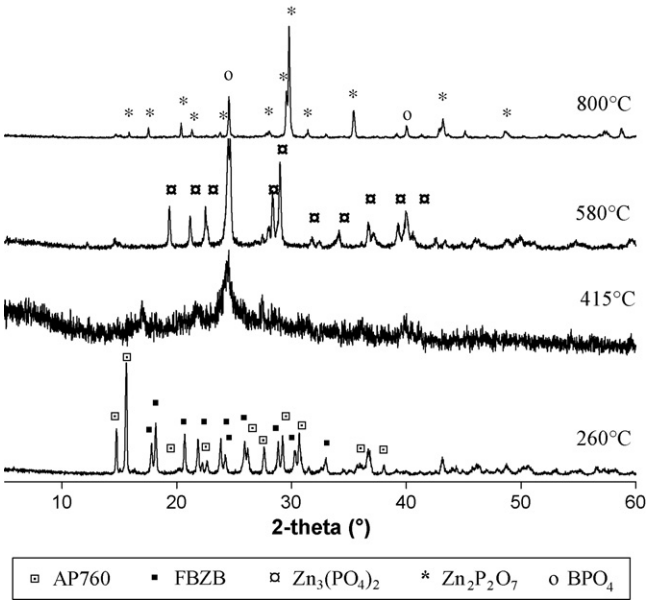

Fig. 11. XRD spectra of the residues of 50/50 AP760/ZB mixtures at the different HTT.

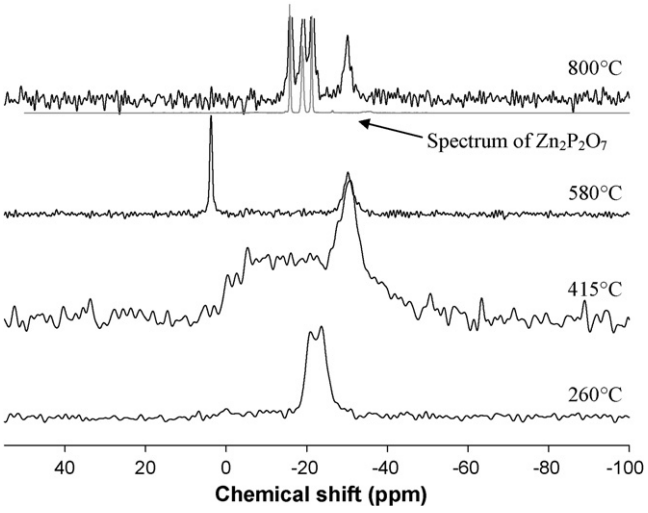

Fig. 13. DD-MAS ^{31}P NMR analyses of the residues.

species [22–24] and certainly to the formation of the phosphocarbonaceous charred structure seen by XRD. The other peaks observed between 14 and 42 ppm are characteristic of aliphatic groups. It can be assigned to aliphatic carbon linked to heteroatom like N or O. For the HTT of 580 °C, the spectra only exhibit a peak of weak intensity around 30 ppm corresponding to aliphatic groups.

The ^{31}P NMR measurements highlighted the degradation of the phosphate species from 415 °C with notably the formation of borophosphates characterised by a band centred at −30 ppm (Fig. 13) [39]. The linewidth in the range (−20;0) ppm is due to a continuous distribution of ^{31}P isotropic chemical shift reflecting the structural disorder such as bond angle and bond length variations and higher coordination sphere disorder. This behaviour may be due to the formation of zinc phosphate because of the chemical shifts typically observed in such glass and because they can be easily formed heating up a mixture of zinc borate and phosphate. At 580 °C, the presence of orthophosphates is also detected (peak at around 3 ppm) [22–24]. It can be assumed that this orthophosphate corresponds to zinc orthophosphate identified by XRD. The phosphorous compound responsible for the three peaks observed at −15.9, −19 and −21.2 ppm in the residue obtained at 800 °C has been identified thanks to the analysis of the reference substance $Zn_2P_2O_7$ and the identification made by XRD. For all spectra, the well defined peaks indicate that the formed products are highly crystallized.

Concerning ^{11}B NMR analyses (Fig. 14), they also proved the evolution of boron species present in the residues. In particular, they confirm the formation of borophosphates from 415 °C (band exhibiting an isotropic chemical shift at −5 ppm) [39]. The evolution of spectra, in the range 0–20 ppm, can be attributed to changes in the BO_3/BO_4 species ratio. The determination of these ratios will be evaluated by NMR simulations presented below.

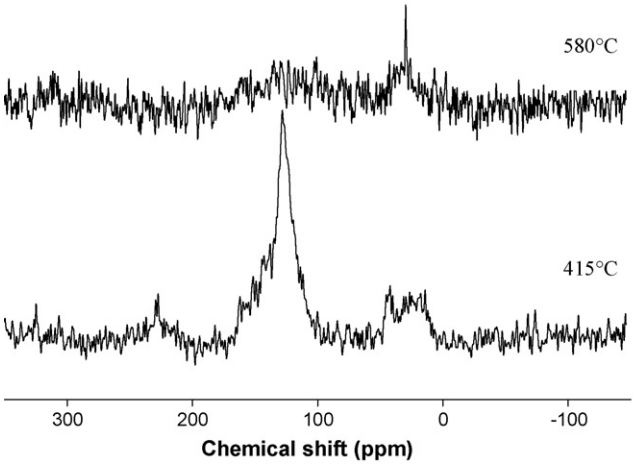

Fig. 12. DD-CP-MAS 13C NMR spectra of AP760/ZB residues at two HTT.

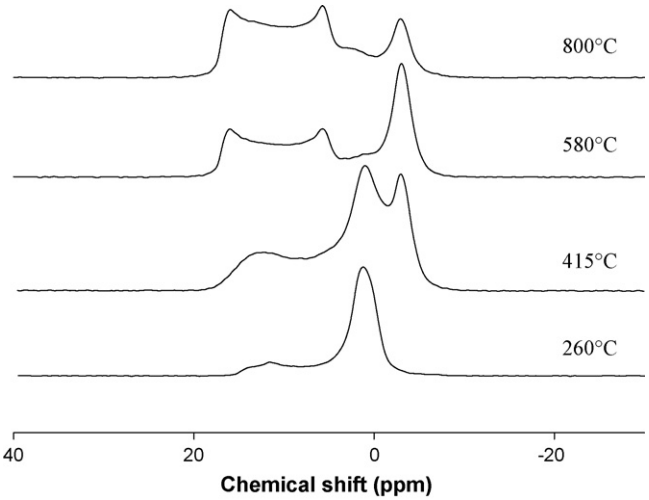

Fig. 14. DD-MAS ^{11}B NMR analyses of the residues.

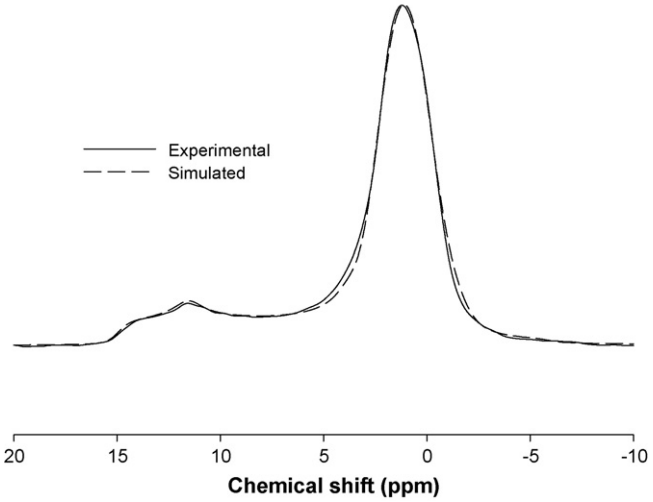

Fig. 15. MAS ^{11}B NMR spectrum of ZB (solid line: experimental spectrum; dotted line: simulated spectrum).

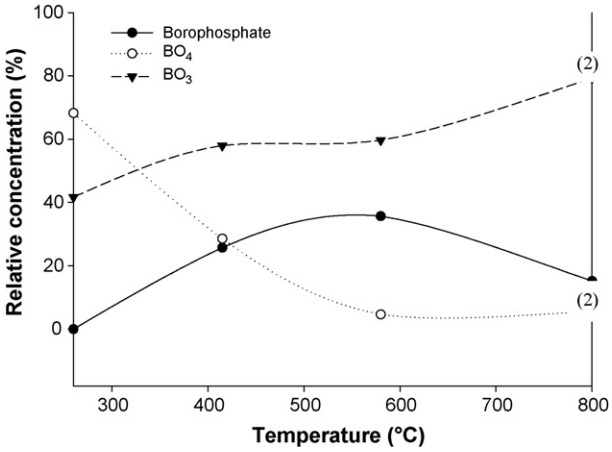

Fig. 16. Evolution of the relative concentration of boron species in AP760/ZB residues vs. temperature; (2) indicates that two different species have been used in the simulation.

NMR simulations have been realised for each residue. An example of simulation is given in Fig. 15 and the characteristic NMR parameters are presented in Table 3.

Depending on the temperature, two, three or five species are detected. Among these species there are two types of BO_4 and BO_3 units and also units corresponding to borophosphates (BP). The proportion of each component in the residues has been evaluated. Their evolution versus the temperature of treatment has been plotted on Fig. 16. The evolution observed is completely different from the evolution of the boron species in neat zinc borate. The BO_4 species decrease exponentially when BO_3 species amount increases almost linearly. At 800 °C two kinds of each unit is used to simulate the spectrum what is probably due to the formation at this temperature of additional BO_3 and BO_4 species with a different surrounding. The borophosphates content reaches a maximum at 580 °C.

3.3.5. Proposed mechanism of degradation

From our experiments (TGA, XRD, NMR of ^{31}P and ^{11}B) the mechanism of degradation of the mixture AP760/ZB might be described as follows. At 260 °C, the two components do not react. The mixture appears like a powder slightly brown what indicates that the degradation of AP760 just begins (Eqs. (1) and (2)); ZB does not undergo any modification (ratio $BO_3/BO_4 = 1/2$). From 290 °C the degradation of ZB starts as described in Eq. (4) leading to an amorphous product. Then the different analyses prove that a reaction between the degradation products of AP760 and ZB occurs between 300 and 415 °C leading to BPO_4 species. Two possible ways of formation of this compound can be suggested (Eqs. (10) and (11)).

$$10(HPO_3)_n + 2ZnO,\ 3B_2O_3 \rightarrow 6BPO_4 + (n-6)/4\,P_4O_{10} + 2ZnO + n/2\,H_2O \quad (10)$$

$$10H_3PO_4 + 2ZnO,\ 3B_2O_3 \rightarrow 6BPO_4 + P_4O_{10} + 2ZnO + 15H_2O \quad (11)$$

The formation of BPO_4 groups may explain the decrease of the content of BO_4 units in the residue observed by NMR since BPO_4 is built up by BO_4 and PO_4 species [40,41] and so the formation of this compound decreases the amount of "free" BO_4. The second way to form the BPO_4 species can explain the aspect of the residue obtained at 415 °C. In fact, the phosphoric acid formed during the degradation of AP760 is responsible for the fatty aspect of the foam obtained dur-

Table 3
NMR parameters of the boron species present in AP760/ZB residues determined by simulation

AP760/ZB 260 °C		AP760/ZB 415 °C			AP760/ZB 580 °C				AP760/ZB 800 °C				
BO_4	BO_3	BO_4	BO_3	BP	BO_4	BO_3	BP	BO_3	BO_4	BO_3	BP	BO_3 (2)	BO_4 (2)
R.C. (%)													
68	32	29	46	25	5	50	36	10	3	67	15	13	2
C_{iso} (ppm)													
2.4	17.2	2.7	18.2	−1.7	2.3	19.7	−1.7	19.7	3.5	19.8	−1.6	17.0	7.1
C_Q													
0.9	2.6	1	2.6	0.9	1	2.5	0.9	2.6	0.9	2.5	0.9	2.5	0.9
η_Q													
0.5	0.3	0.8	0.3	0.6	0.1	0	0.8	0.3	0.4	0	0.8	0.2	0.8

R.C.: Relative concentration.

ing the degradation of AP760. But the residue at 415 °C has not a fatty aspect and it can be explained by the immediate consumption of the phosphoric acid to yield BPO_4. In the residue, another phase containing boron species is also detected by NMR. This species can be unreacted 2ZnO, $3B_2O_3$ what could explain the amorphous phase detected by XRD. To explain the formation of the compound $Zn_3(PO_4)_2$ at 580 °C, a reaction between the zinc oxide and P_4O_{10} (two compounds formed in the step before) can be suggested as indicated on Eq. (12).

$$3ZnO + 0.5P_4O_{10} \rightarrow Zn_3(PO_4)_2 \quad (12)$$

The zinc orthophosphate is a product which melts at about 1050 °C to yield zinc oxide and P_2O_5 (Eq. (13)).

$$Zn_3(PO_4)_2 \xrightarrow{1050^\circ C} 3ZnO + P_2O_5 \quad (13)$$

This degradation might occur at lower temperature depending on the time of the thermal treatment. In this case the degradation products could react to yield the zinc pyrophosphate (Eq. (14)).

$$2ZnO + 3P_2O_5 \rightarrow Zn_2P_2O_7 \quad (14)$$

The mechanisms exposed above do not explain the disappearing of BPO_4. So another mechanism should be proposed. This mechanism is only based on our results. It can be suggested that the zinc orthophosphate reacts with the borophosphates to lead zinc pyrophosphate and the compound B_2O_3 as described in the Eq. (15).

$$2Zn_3(PO_4)_2 + 2BPO_4 \rightarrow B_2O_3 + 3Zn_2P_2O_7 \quad (15)$$

The formation of B_2O_3 could explain the increase of the BO_3 species seen by ^{11}B NMR since B_2O_3 is built up by BO_3 triangles.

4. Conclusion

In this work, the degradation of AP760/ZB mixture has been investigated in comparison with the degradation of the two compounds taken separately using TGA and solid state NMR and XRD analyses. It has been demonstrated that reactions occur between AP760 and ZB leading to the formation of borophosphates and zinc phosphates which stabilize phosphorous species. The different analyses have enabled to propose a detailed mechanism explaining the degradation and the interactions of the mixture AP760/ZB. This study presents a practical interest in the flame retardant field. AP760 is an intumescent flame retardant formulations and another study made in our laboratory has revealed the presence of a synergistic effect by adding ZB in the polypropylene/AP760 formulations. This study should then permit us to explain this phenomenon.

Acknowledgements

The authors thank Luzenac for its financial support. They are indebted to Pascal Amigouët, Frederic Jouffret and Kelvin Shen for their helpful discussions and their contribution to this study and to Bertrand Revel (Centre Commun de Mesures RMN de l'Université des Sciences et Technologies de Lille) for his skilful experimental assistance in NMR.

References

[1] C.L. Christ, J.R. Clark, Phys. Chem. Miner. 2 (1977) 59–87.
[2] P.C. Burns, J.D. Grice, F.C. Hawthorne, Can. Mineral. 33 (1995) 1131–1142.
[3] P.C. Burns, Can. Mineral. 33 (1995) 1167–1176.
[4] J.D. Grice, P.C. Burns, F.C. Hawthorne, Can. Mineral. 37 (1999) 731–742.
[5] C. Chen, Y. Wang, B. Wu, K. Wu, W. Zeng, L. Yu, Nature 373 (1995) 322.
[6] D.M. Schubert, F. Alam, M.Z. Visi, C.B. Knobler, Chem. Mater. 15 (2003) 866–871.
[7] http://www.borax.com.
[8] K. Shen, E. Olson, Proceedings – American Chemical Society Meeting, Philadelphia, PA, August 22–26, 2004.
[9] S. Bourbigot, M. LeBras, S. Duquesne, in: M. LeBras, S. Bourbigot, S. Duquesne, C. Jama, C. Wilkie (Eds.), Fire Retardancy of Polymers, The Royal Society of Chemistry, 2005, pp. 327–335.
[10] S. Bourbigot, F. Carpentier, M. Le Bras, C. Fernandez, J.P. Amoureux, R. Delobel, Extended Abstracts – EUROFILLERS 97, International Conference on Filled Polymers and Fillers, 2nd, Manchester, UK, Sept. 8–11, 1997, 419–423.
[11] S. Bourbigot, M. Le Bras, R. Leeuwendal, K. Shen, D. Schubert, Polym. Degrad. Stab. 64 (3) (1999) 419–425.
[12] F. Carpentier, S. Bourbigot, M. Le Bras, R. Delobel, Polym. Int. 49 (10) (2000) 1216–1221.
[13] S. Bourbigot, M. Le Bras, S. Duquesne, M. Rochery, Macromol. Mater. Eng. 289 (2004) 499–511.
[14] S. Bourbigot, M. le Bras, S. Duquesne, European Meeting on Fire Retardancy and Protection of Materials, 9th, Lille, France, Sept. 17–19, 2003, 327–335.
[15] M. Hellenbrandt, Crystallogr. Rev. 10 (1) (2004) 17–22.
[16] J.P. Amoureux, C. Fernandez, L. Carpentier, E. Cochon, Phys. Stat. Sol. 132 (1992) 461–475.
[17] G. Camino, M.P. Luda, R. Soc. Chem. 224 (1998) 48–63.
[18] C. Drevelle, S. Duquesne, M. Le Bras, J. Lefebvre, R. Delobel, A. Castrovinci, C. Magniez, M. Vouters, JAPS 94 (2) (2004) 717–729.
[19] S. Bourbigot, M. Le Bras, R. Delobel, Carbon 33 (3) (1995) 283–294.
[20] M. Le Bras, S. Bourbigot, Y. Le Tallec, J. Laureyns, Polym. Degrad. Stab. 56 (1) (1997) 11–21.
[21] S. Bourbigot, M. Le Bras, F. Dabrowski, J.W. Gilman, T. Kashiwagi, Fire Mater. 24 (4) (2000) 201–208.
[22] M. Bugajny, S. Bourbigot, M. Le Bras, R. Delobel, Polym. Int. 48 (1999) 264–270.
[23] S. Bourbigot, F. Carpentier, M. Le Bras, C. Fernandez, Polym. Addit., chapitre 14 (2001) 271.
[24] A. Marchal, R. Delobel, M. Le Bras, J.-M. Leroy, D. Price, Polym. Degrad. Stab. 44 (1994) 263–272.
[25] A.H. Silver, P.J. Bray, J. Chem. Phys. 29 (1958) 984–990.
[26] P.J. Bray, J.O. Edwards, J.G. O'Keefe, V.F. Ross, I. Tatsuzaki, J. Chem. Phys. 35 (1961) 435–442.
[27] P.J. Bray, Inorg. Chim. Acta 289 (1999) 158–173.
[28] G.L. Turner, K.A. Smith, R.J. Kirkpatrick, E. Oldfield, J. Magn. Reson. 67 (1986) 544–550.
[29] D. Müller, A.R. Grimmer, U. Timper, G. Heller, M.Z. Shakibai-Moghadam, Z. Anorg. Allg. Chem. 619 (1993) 1262–1268.
[30] L. Van Wüllen, W. Mueller-Warmuth, D. Papageorgiou, H.J. Penthinghaus, J. Non-Cryst. Solids 171 (1994) 53–67.
[31] J.F. Stebbins, P. Zhao, S. Kroecker, Solid State Nucl, Magn. Reson. 16 (2000) 9–19.
[32] R. Martens, W. Müller-Warmuth, J. Non-Cryst. Solids 265 (2000) 167–175.
[33] S. Kroeker, J.F. Stebbins, Inorg. Chem. 40 (2001) 6239–6246.

[34] M.R. Hansen, T. Vosegaard, H.J. Jakobsen, J. Skibsted, J. Phys. Chem. A 108 (2004) 586–594.
[35] http://mutuslab.cs.uwindsor.ca/schurko/ssnmr/ssnmr_schurko.pdf.
[36] H. Huppertz, G. Heymann, Solid state sci. 5 (2003) 281–289.
[37] H. Bauer, Z. Anorg. Allg. Chem. 320 (1963) 306–316.
[38] A. Whitaker, J. Mat. Sci. 7 (1972) 189–193.
[39] A.-R. Grimmer, D. Müller, G. Gözel, R. Kniep, Fresenius J. Anal. Chem. 357 (1997) 485–488.
[40] S.N. Achary, A.K. Tyagi, J. Solid State Chem. 177 (2004) 3918–3926.
[41] F.A. Hummel, T.A. Kupinski, J. Am. Chem. Soc. 72 (1950) 5318–5319.